13th World Conference on Earthquake Engineering
Vancouver, B.C., Canada
August 1-6, 2004
Paper No. 3482

A STUDY ON THE SEISMIC FORCE RESISTING MECHANISM OF A MULTI-STORY SHEAR WALL SYSTEM CONSIDERING THE INTERACTION BETWEEN WALL, SLAB, FOUNDATION BEAM, AND PILE ELEMENTS

Masanobu Sakashita[1], Hakim Bechtoula[2], Susumu Kono[3], Hitoshi Tanaka[4], Fumio Watanabe[5]

SUMMARY

Two 1/5 scale specimens were designed and constructed as basic structural assemblage models extracted from a practical six-story shear wall system. Those specimens consisted of a bottom two-story part of the shear wall system, a foundation beam, slabs, and two piles. Static lateral load was applied with proportionally varying vertical load to simulate loading conditions of the prototype six-story shear wall system under earthquakes.
The foundation beam resisted by itself and the contribution from the piles and shear wall was less than expected. This caused unexpected shear cracking to spread extensively over the foundation beam. However, longitudinal bars in slabs worked together with the upper longitudinal reinforcement in the foundation beam. Transition of shear transfer mechanisms at the shear wall base was observed from the strain distribution of longitudinal reinforcement in foundation beams and those strain distributions of different loading stage were predicted accurately. The lateral load–drift relations obtained experimentally was simulated well with a simple superposition of flexure and shear elements.

INTRODUCTION

In current design procedures [1][2], cantilever structural walls are normally assumed to stand on a solid foundation, and the foundation beams, slabs and piles are designed separately without considering their interactions. This is because their interactions have not been thoroughly studied for its complexity. Also neglected in the practical design is the fact that shear transfer mechanisms along the wall base vary depending on the crack patters and inelastic deformation levels at the shear wall base. This study aims to experimentally clarify the variation of the lateral load resisting mechanisms considering the interaction between a shear wall, foundation beams, slabs and piles, and to establish more rational design procedures for each structural component.

---

[1] PhD candidate, Dept.of Architecture, Kyoto University, Japan. Email: rc.sakashita@archi.kyoto-u.ac.jp
[2] PhD candidate, Dept.of Architecture, Kyoto University, Japan.
[3] Associate Professor, Dept.of Architecture, Kyoto University, Japan. Email: kono@archi.kyoto-u.ac.jp
[4] Professor, Dept.of Architecture, Kyoto University, Japan
[5] Professor, Dept.of Architecture, Kyoto University, Japan

In the experimental program, the specimen configuration was determined from typical six story residential buildings in Japan. They normally have multiple spans of a RC moment resisting frame in the longitudinal direction and a single span of shear wall system in the transverse direction. In this study, the assemblage consisting of the lowest two floors of shear wall with a foundation beam, the first floor slab, and two piles in the transverse direction was scaled to 1/5 to make model specimens. The shear wall was designed to fail in flexure and the shear span ratio of the piles was fixed as 2.2 although the shear span ratio is supposed to vary depending on the soil, axial force, and lateral force under earthquakes.

EXPERIMENTAL SETUP

Specimens and test setup

Figure 1(a) shows specimen configuration. The first floor slab extended 600 mm on either side of the wall and the total width was 1200mm. The shear wall and the slabs had the same thickness of 60mm. The piles were designed to be elastic and extended to the top surface of the foundation beam so that the sufficient lateral force can be transferred to the foundation beam. The center-to-center distance of the piles was 1800mm. The distance between the supporting pins and the top edge of the slab was set 1240mm. Two specimens were identical except that they had different amount of longitudinal bars in the foundation beam. As shown in Table 2(b), the yielding of the foundation beam was designed to precede the yielding of the shear wall for FLB16 and vice verse for FLB13. The foundation beam of FLB16 had eight D16 longitudinal reinforcing bars as shown in Figure 1(b) while that of FLB13 had eight D13 bars instead. Both specimens had eight D10 bars spliced to these longitudinal bars for 400mm long at the midspan as shown in Figure 1(b) to simulate the bar cutoff in practice. Material properties are shown in Table 1.

Table 1: Material properties of concrete and bars

(a) Concrete

	Compressive strength (MPa)	Tensile strength (MPa)	Young's modulus (GPa)
Foundation beam, Pile	30.5	2.82	22.4
Wall, Column, Beam	29.1	3.04	24.8

(b) Steel reinforcement

	Yield strength (MPa)	Young's modulus (GPa)	Tensile strength (MPa)
φ4	518	198	562
D10	341	161	452
D13	327	197	510
D16	334	201	530

Table 2: Types of reinforcement and test values

(a) Type of reinforcement

Member	Type of bars		Steel ratio (%)
Column (160×160mm)	Longitudinal	4-D10	1.40
	Transverse	2-φ4@80	0.21
Beam (120×160mm)	Longitudinal	4-D10	1.74
	Transverse	2-φ4@50	0.42
Shear Wall (Thickness 60mm)	Vertical	φ4@80	0.26
	Horizontal	φ4@80	0.26
Pile (350×350mm)	Longitudinal	8-D22	2.48
	Transverse	4-D10@100	0.90

(b) Test Variables

Member	Bars		Steel ratio (%)
Foundation beam (FLB16) (150×480mm)	Longitudinal	4-D16	2.24
	Transverse	2-D10@100	1.05
	Flexural yield strength	64MPa	
Foundation beam (FLB13) (150×480mm)	Longitudinal	4-D13	1.48
	Transverse	2-D10@100	1.05
	Flexural yield strength	101MPa	

66MPa is the moment acting on the foundation beam when the shear wall yields in flexure.

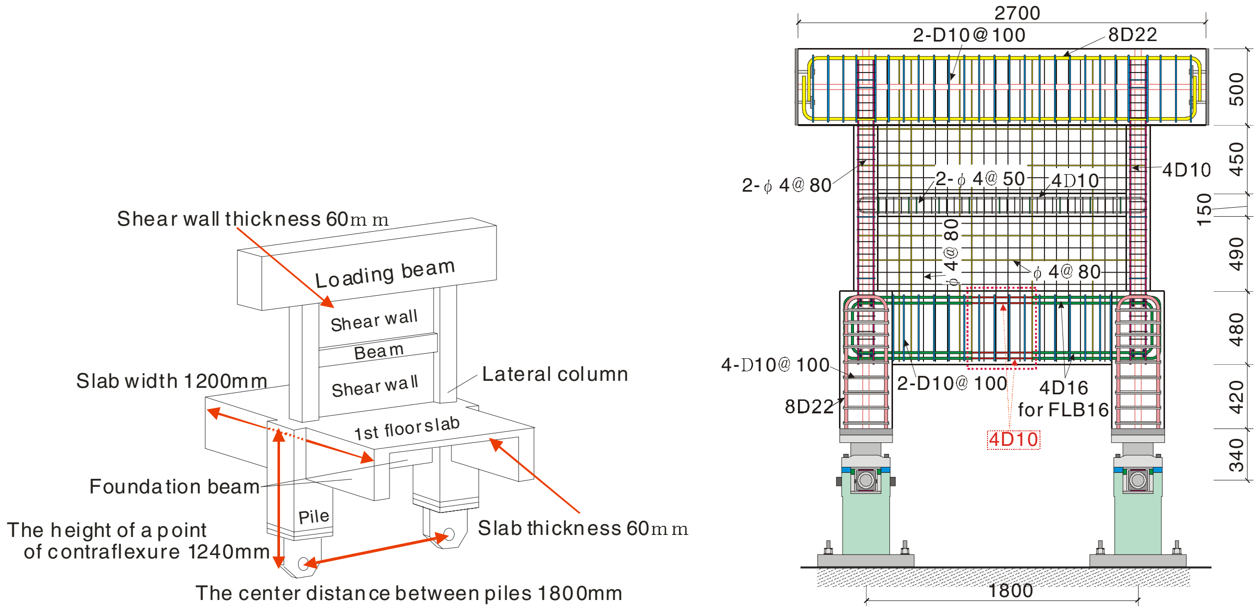

(a) Specimen configuration **(b) Reinforcement for FLB16**

Figure 1: Specimen configuration and reinforcement arrangement

As shown in Figure 2, lateral load, Q, was applied statically through a 1000kN horizontal jack to the loading beam. Four vertical jacks were adjusted to create appropriate column axial forces, N1 and N2, which are a liner function of lateral load, Q, to simulate loading conditions of the prototype six-story shear wall system under earthquakes.

$$N_1 \ and \ N_2 = 72 \pm 0.63 \cdot Q \qquad (kN) \qquad (1)$$

At the roller support, Q/2 was applied horizontally to the pile by a 500kN jack in the opposite direction to the 1000kN jack. This causes the possible maximum axial force in the foundation beams at the ultimate stage assuming the mechanism in Figure 11 where large rotation of the shear wall makes the shear force Q transfer through the limited area under compression. The load was applied two cycles at each prescribed load stage until the shear wall yielded, then the displacement control was used with two cycles at each prescribed displacement. As shown in Figure 2, the story drift angle of the first floor was measured with a displacement gauge on a measurement frame that was fixed to the transverse foundation beams.

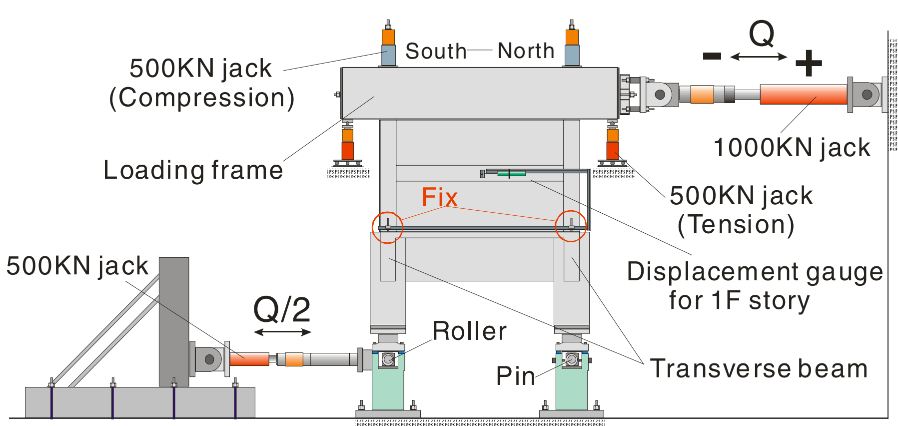

Figure 2: Loading system

ANALYTICAL PROGRAM

Prediction of load-displacement relationship

The lateral load-drift angle relations of shear walls were simulated using a simple model. The model employs a superposition of flexure and shear actions. The flexural action was modeled with an ordinary flexural element based on a beam theory and the shear action was modeled using Hirata et al.'s model [3]. As shown in Figure 8, the envelope curves of the flexural element and the shear element were assumed tri-linear. Figure 4 compares the calculated curves and experimental results. The characteristic points are summarized in Table 3. The computed flexural cracking strengths were smaller than the experimental results and computed flexural strengths agreed well with the experimental results.

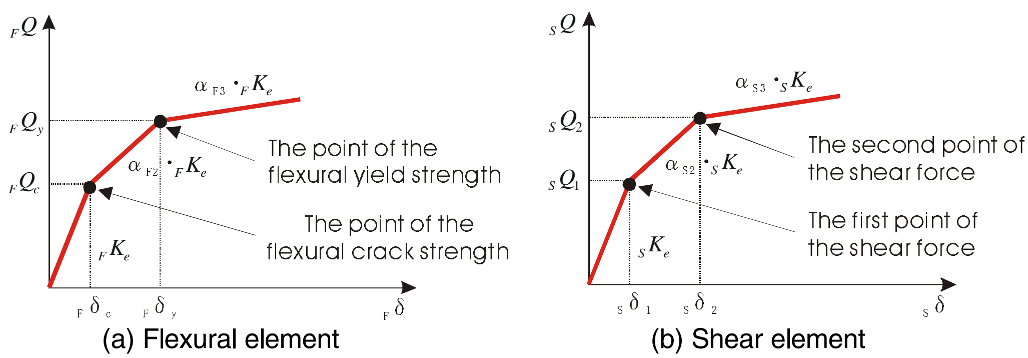

Figure 8: Shear force – drift relations for the flexural element and shear element

Table 3: Cracking and yielding strengths in flexure

	analysis	FLB16		FLB13	
		positive	negative	positive	negative
Flexural crack strength,Qcr (kN)	108	134		147	
Story drift at Qcr (%)	0.006	0.056		0.059	
Flexural yield strength, Qy (kN)	180.0	173	-175	167	-154
Story drift at Qy (%)	0.194	0.388	-0.130	0.558	-0.084

Simulation of strain distributions of the foundation beam before and after the shear wall yielded

Figure 9 shows a model to analyze the foundation beam. The foundation beam is subjected to moment from the piles (Mp), and moment (Mq) and axial force due to lateral force, Q, acting on the upper edge of the foundation beam. The distributions of Mq and N vary as the shear wall rotates and the contacting area between the shear wall and the foundation beam decreases. Figure 10 shows a schematic figure of contact and detachment of the foundation base. Numbers beside each figure indicate the degree of detachment.

If Q distributed uniformly across the whole shear wall base, Mp and N can be computed as shown in Figure 9. It is assumed that the shear wall rotates and applied Q is transferred through a region under compression as shown in Figure 11. Figure 11 shows the models of the distributions of Mq and N corresponding to the degree of detachment in Figure 10.

Using the models in Figure 9 and Figure 11, the strain distributions of the longitudinal reinforcement in the foundation beam were computed at the three loading stages in Figure 4. It should be noted that D10 bars were spliced to D13 or D16 bars at 400 mm of midspan and the strain distribution is discontinuous in this region.

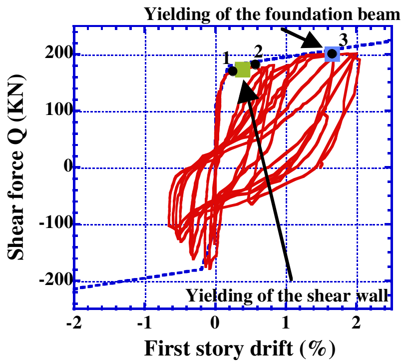

(a) FLB16

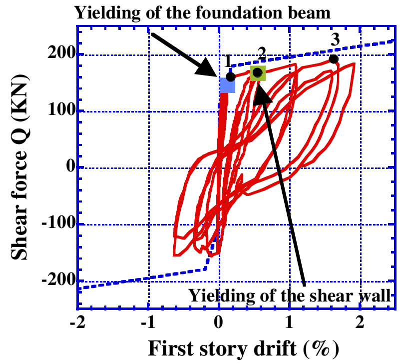

(b) FLB13

Figure 4: Lateral load - first story drift relations

Strain distributions of longitudinal reinforcement in the foundation beam and in the slabs

Figure 5 and Figure 6 show the strain distribution of longitudinal bars in the foundation beams. Three lines in each numbers in Figure 5 and Figure 6 show the distribution for three stages shown in Figure 4.

Outside of D10 region, strains for FLB13 in Figure 6(a) tended to be higher than that for FLB16 in Figure 5(a) since the flexural yielding of the foundation beam preceded the flexural yielding of the shear wall in FLB13. The negative (south) side location, strains of FLB13 increased from Stage 2 to Stage 3 probably because the shear cracking cause the debonding and the tension shift penetrated to the south side.

It is also noted that at the end region near +600mm in Figure 5(a) and Figure 6(a), the strains are lower than the expected linear distribution extrapolated from strains of inner region. On the other hand, near -600mm in Figure 5(b) and Figure 6(b), the strains are linearly distributed as expected from the extrapolation. Then the restrained strains of upper longitudinal reinforcement can be attributed to the constraint from the slabs and the shear wall but not to the tension shift from shear cracking. Upper reinforcement seems to have more influence on the change of lateral load resisting mechanism than the lower reinforcement since distributions of strain at three stages are distinctively different. This phenomenon is expressed later in Figure 11.

Figure 5(c) and Figure 6(c) show the average strain distribution of longitudinal bars in slabs and Figure 7 shows the cross section of the foundation beam and the slabs. Each strain distribution in those figures agreed well with the strain distribution at the same stage in Figure 5(a) and Figure 6(a). Since longitudinal bars in the slabs at a certain section showed nearly identical strain readings, the whole width of the slabs can be considered effective.

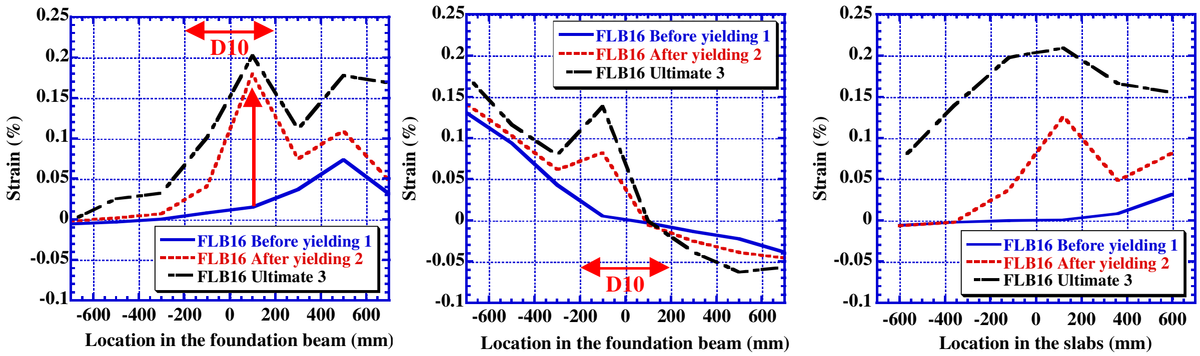

(a) Upper longitudinal bar (Foundation beam) (b) Lower longitudinal bar (Foundation beam) (c) longitudinal bars (Slabs)

Figure 5: Strain distributions of reinforcement for FLB16

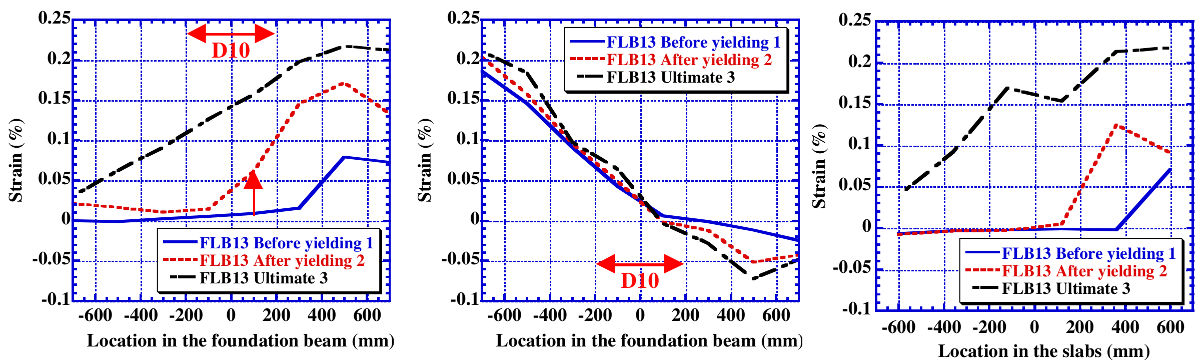

(a) Upper longitudinal bar (Foundation beam) (b) Lower longitudinal bar (Foundation beam) (c) longitudinal bars (Slabs)

Figure 6: Strain distributions of reinforcement for FLB13

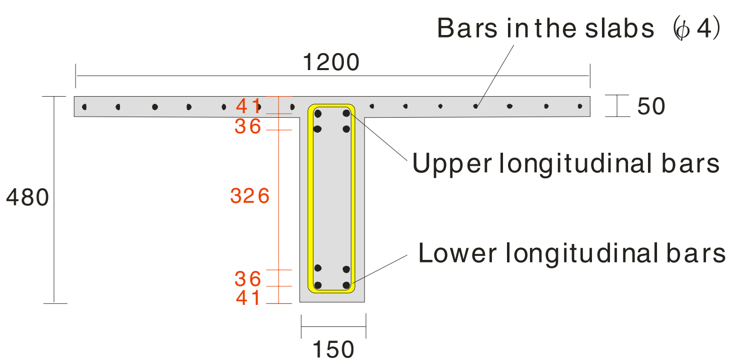

Figure 7: The cross section of the foundation beam and the slabs

ANALYTICAL PROGRAM

Prediction of load-displacement relationship

The lateral load-drift angle relations of shear walls were simulated using a simple model. The model employs a superposition of flexure and shear actions. The flexural action was modeled with an ordinary flexural element based on a beam theory and the shear action was modeled using Hirata et al.'s model [3]. As shown in Figure 8, the envelope curves of the flexural element and the shear element were assumed tri-linear. Figure 4 compares the calculated curves and experimental results. The characteristic points are summarized in Table 3. The computed flexural cracking strengths were smaller than the experimental results and computed flexural strengths agreed well with the experimental results.

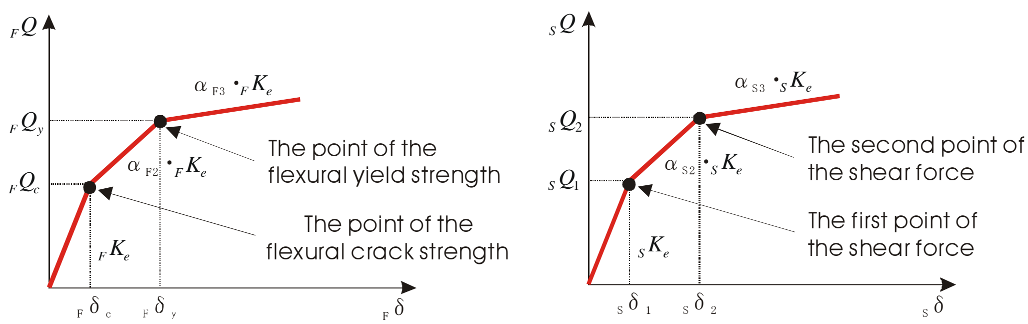

(a) Flexural element (b) Shear element

Figure 8: Shear force – drift relations for the flexural element and shear element

Table 3: Cracking and yielding strengths in flexure

	analysis	FLB16		FLB13	
		positive	negative	positive	negative
Flexural crack strength,Qcr (kN)	108	134		147	
Story drift at Qcr (%)	0.006	0.056		0.059	
Flexural yield strength, Qy (kN)	180.0	173	-175	167	-154
Story drift at Qy (%)	0.194	0.388	-0.130	0.558	-0.084

Simulation of strain distributions of the foundation beam before and after the shear wall yielded

Figure 9 shows a model to analyze the foundation beam. The foundation beam is subjected to moment from the piles (Mp), and moment (Mq) and axial force due to lateral force, Q, acting on the upper edge of the foundation beam. The distributions of Mq and N vary as the shear wall rotates and the contacting area between the shear wall and the foundation beam decreases. Figure 10 shows a schematic figure of contact and detachment of the foundation base. Numbers beside each figure indicate the degree of detachment.

If Q distributed uniformly across the whole shear wall base, Mp and N can be computed as shown in Figure 9. It is assumed that the shear wall rotates and applied Q is transferred through a region under compression as shown in Figure 11. Figure 11 shows the models of the distributions of Mq and N corresponding to the degree of detachment in Figure 10.

Using the models in Figure 9 and Figure 11, the strain distributions of the longitudinal reinforcement in the foundation beam were computed at the three loading stages in Figure 4. It should be noted that D10 bars were spliced to D13 or D16 bars at 400 mm of midspan and the strain distribution is discontinuous in this region.

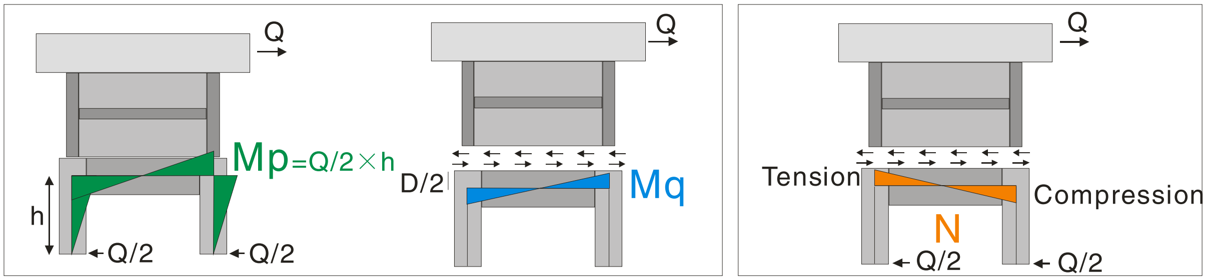

(a) Moment from piles (b) Moment due to lateral force (c) axial force due to lateral force

Figure 9: Moment and axial force acting on the foundation beam

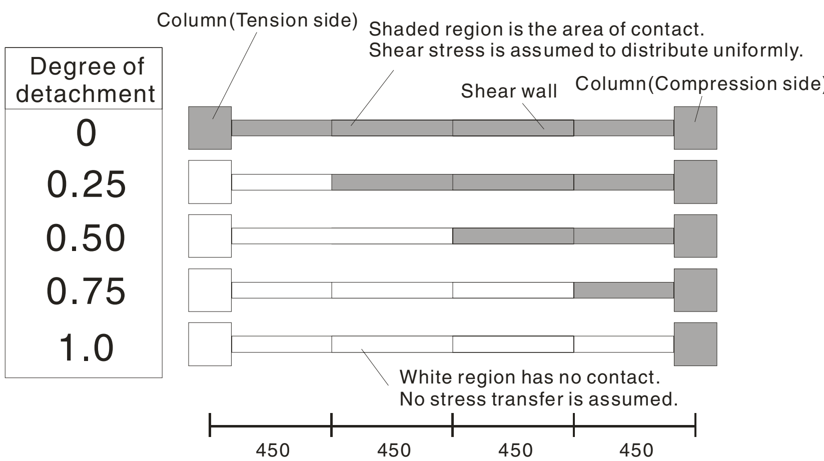

Figure 10: The regions where the shear wall lifts up

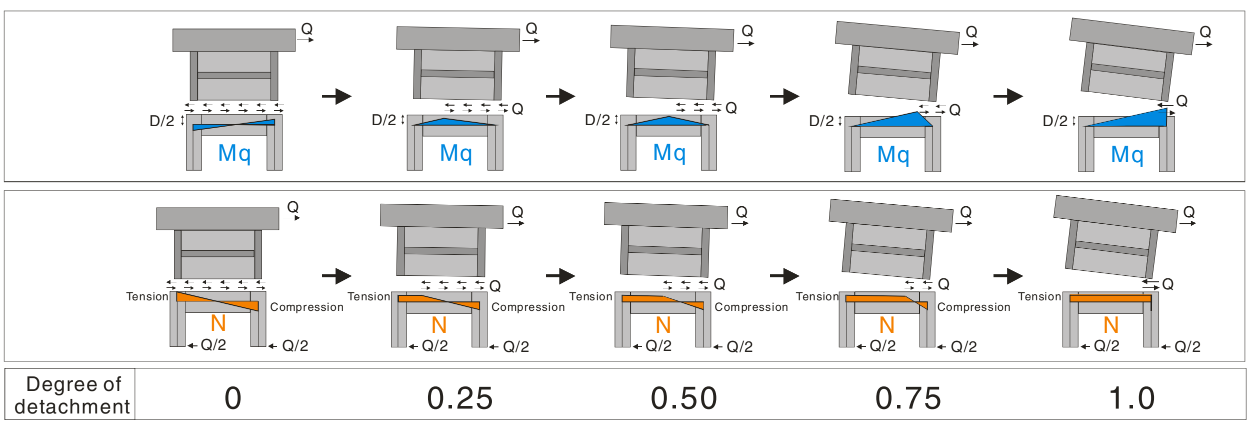

(a) DD=0 (b) DD=0.25 (c) DD=0.50 (d) DD=0.75 (e) DD=1.0

Figure 11: Distributions of Mq and N corresponding to the degree of detachment (DD)

Figure 12 shows the comparison between the computed and experimental strain distributions of FLB16. Contribution of reinforcing bars in the slabs is considered in the computed. Lines 0, 0.25, 0.50, 0.75 and 1.0 indicate the strain distributions corresponding to the degree of detachment in Figure 10 and Figure 11.

When the shear wall yielded, the strains of the upper longitudinal bars rapidly increased at midspan. This is because the distribution of moment shifts from Figure 11(a) to Figure 11(b) or (c). Without the region near –100mm in lower longitudinal bars, the computed strain distributions agreed well with experimental results.

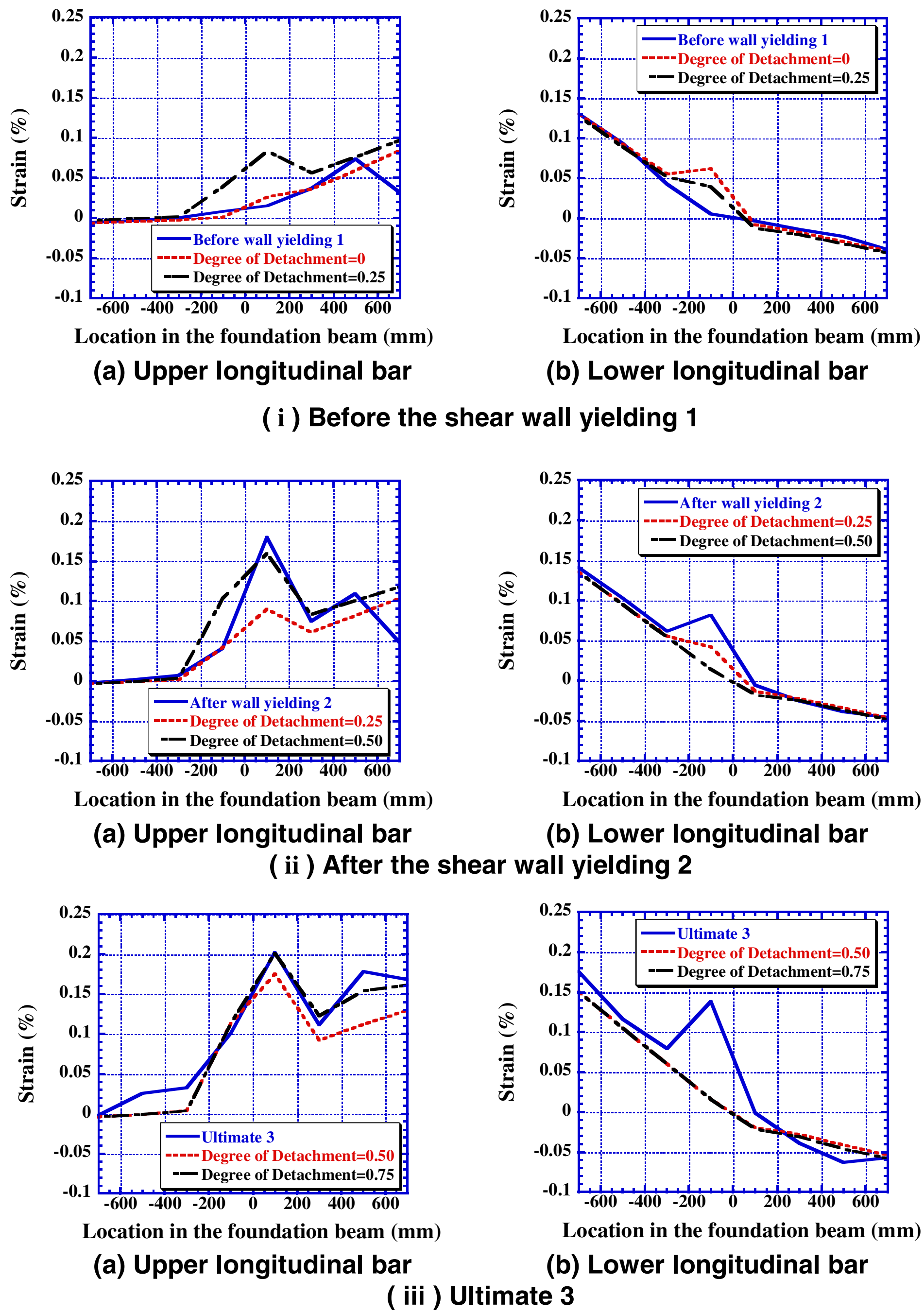

Figure 12: Strain distributions of longitudinal reinforcement of FLB16

CONCLUSIONS

Two 1/5-scale cantilever structural wall systems were tested to clarify the variation of the lateral load resisting mechanisms considering the interaction between a shear wall, foundation beams, slabs and piles. The main conclusions can be summarized as follows.

- Monolithic action between foundation beam and peripheral members, such as shear wall and piles, was much less than expected and unexpected shear cracking spread extensively over the foundation beam. However, longitudinal bars in slabs worked together with the upper longitudinal reinforcement in the foundation beam. As designed a priori, the shear wall of FLB16 had more damage than that of FLB13.

- Strain distributions of longitudinal reinforcement in foundation beams from experiment and analysis show the shear transfer mechanism clearly. In the analysis, it is assumed that the foundation beam is subjected to moment from the piles (Mp), and moment (Mq) and axial force due to lateral force, Q, acting on the upper edge of the foundation beam.

- Lateral load – drift relations can be simulated well with a simple superposition of flexural and shear elements.

REFERENCES

[1] Architecture Institute of Japan, "AIJ Standard for Structural Calculation of Reinforced Concrete Structures Based on Allowable Stress Concept," 1999, pp218-241.

[2] Paulay, T. and Priestley, M.J.N., "Seismic Design of Reinforced Concrete and Mansonry Buildings," John Wiley & Sons, 1992, pp. 362-499.

[3] Hirata, M., Naraoka, S., Kim, Y., Sanada, Y., Matsumoto, K., Kabeyazawa, T., Kuramoto, H., Hukuda, T., Kato, A., Ogawa, M., "Dynamic Test of Reinforcement Concrete Wall-Frame System with Soft First Story Part 1-Part 4" Summaries of technical papers of annual meeting architectural institute of Japan, 2001,pp705-712 (in Japanese).